Letter

Decoding the nature of $Z_{cs}(3985)$ and establishing the spectrum of charged heavy quarkoniumlike states in chiral effective field theory

Bo Wang,[1,2] Lu Meng,[3,*] and Shi-Lin Zhu[1,2,†]

[1]*Center of High Energy Physics, Peking University, Beijing 100871, China*
[2]*School of Physics and State Key Laboratory of Nuclear Physics and Technology, Peking University, Beijing 100871, China*
[3]*Ruhr University Bochum, Faculty of Physics and Astronomy, Institute for Theoretical Physics II, D-44870 Bochum, Germany*

(Received 24 November 2020; accepted 10 December 2020; published 7 January 2021)

We study the newly observed charmoniumlike state $Z_{cs}(3985)$ in the framework of chiral effective field theory. The interaction kernel of the $\bar{D}_s D^*/\bar{D}_s^* D$ system is calculated up to the next-to-leading order with the explicit chiral dynamics. With the fitted parameters extracted from the $Z_c(3900)$ data as inputs, the mass, width, and event distributions of the $Z_{cs}(3985)$ are very consistent with the experimental measurements. Our studies strongly support the $Z_{cs}(3985)$ as the partner of the $Z_c(3900)$ in the $\mathrm{SU}(3)_f$ symmetry and the $\bar{D}_s D^*/\bar{D}_s^* D$ molecular resonance with the same dynamical origin as the other charged heavy quarkoniumlike states. We precisely predict the resonance parameters of the unobserved states in $\bar{D}_s^* D^*$, $B_s^* \bar{B}/B_s \bar{B}^*$, and $B_s^* \bar{B}^*$ systems, and establish a complete spectrum of the charged charmoniumlike and bottomoniumlike states with the $I(J^P)$ quantum numbers $1(1^+)$ and $\frac{1}{2}(1^+)$, respectively.

DOI: 10.1103/PhysRevD.103.L021501

I. INTRODUCTION

Very recently, the BESIII Collaboration observed a new charged charmoniumlike state $Z_{cs}(3985)$ in the K^+ recoil-mass spectrum from the process $e^+e^- \to K^+(D_s^- D^{*0} + D_s^{*-} D^0)$ at the center-of-mass energy $\sqrt{s} = 4.681$ GeV [1]. Its mass and width were measured to be $M_{Z_{cs}}^{\mathrm{pole}} = (3982.5^{+1.8}_{-2.6} \pm 2.1)\,\mathrm{MeV}$ and $\Gamma_{Z_{cs}}^{\mathrm{pole}} = (12.8^{+5.3}_{-4.4} \pm 3.0)\,\mathrm{MeV}$, respectively. The minimal quark component in $Z_{cs}(3985)^-$ should be $c\bar{c}s\bar{u}$ rather than the pure $c\bar{c}$ since it is a charged particle with strangeness. The mass of $Z_{cs}(3985)$ is about 100 MeV larger than that of the $Z_c(3900)$, which is the typical mass difference between the $D_s^{(*)}$ and $D^{(*)}$ mesons [2]. Another salient feature of $Z_{cs}(3985)$ is the closeness to the $\bar{D}_s D^*/\bar{D}_s^* D$ threshold. It is proposed in Ref. [3] that the newly observed $Z_{cs}(3985)^-$ is the U-spin partner of $Z_c(3900)^-$ under the $\mathrm{SU}(3)_f$ symmetry. The $Z_{cs}(3985)$ has been intensively studied within a very short time [4–10].

There are large similarities among $Z_{cs}(3985)$ [1], $Z_c(3900)$ [11], $Z_c(4020)$ [12], $Z_b(10610)$, and $Z_b(10650)$ [13] (we will denote these states as Z_{cs}, Z_c, Z_c', Z_b, and Z_b', respectively, in the following context for simplicity). They all lie few MeVs above the corresponding $\bar{D}_s D^*$, $D\bar{D}^*$, $D^*\bar{D}^*$, $B\bar{B}^*$, and $B^*\bar{B}^*$ thresholds, respectively. They dominantly decay into the open charm/bottom channels [14]. In our recent work [15], we studied the interactions of the isovector $D^{(*)}\bar{D}^{(*)}$ and $B^{(*)}\bar{B}^{(*)}$ systems with the chiral effective field theory (χEFT) up to the next-to-leading order. We find the invariant mass spectra of the open charm/bottom channels can be described well and the peaks originate from the poles in the unphysical Riemann sheet. In other words, the previously observed $Z_Q^{(\prime)}$ states can be well identified as the dynamically generated molecular resonances from the $D^{(*)}\bar{D}^{(*)}$ and $B^{(*)}\bar{B}^{(*)}$ interactions. The large similarity between the Z_{cs} and $Z_Q^{(\prime)}$ stimulates us to wonder whether the newly observed Z_{cs} has the same origin. This paper is devoted to answering this question.

The discoveries of more and more near-threshold exotic states [14,16–20] indicate some common features of QED and QCD. For the very near-threshold bound states and resonances, physical observables are insensitive to the details of the interaction, which yields universality in both hadronic and atomic sectors [21]. Meanwhile, the hadronic molecules arise from the residual strong interactions

*lu.meng@rub.de
†zhusl@pku.edu.cn

between two color singlet objects, which is analogous to molecules bound by the residual interaction of QED. The separable scales in these near-threshold states lead to a feasible approach to improvable expansion, which is the basic idea of effective field theory.

The χEFT is generally accepted as the modern theory of nuclear forces [22–28], which is built upon two pioneer works of Weinberg [29,30], and has been successfully applied to describe the low energy NN scatterings, light and medium nuclei [23–25]. Recently, we generalized the framework of χEFT to the systems with heavy quarks and reproduced the hidden-charm pentaquarks successfully [31,32]. Within χEFT, we predicted the existence of strange hidden charm molecular pentaquarks P_{cs} in the isoscalar $\Xi_c\bar{D}^*$ system [33]. Our prediction was confirmed by the new measurement of LHCb at the $J/\psi\Lambda$ final state [34]. Therefore, it is reliable to utilize the χEFT to depict the chiral dynamics inside the $\bar{D}_sD^*/\bar{D}_s^*D$ systems, likewise. The investigation could be extended further to Z_{cs}' in the $\bar{D}_s^*D^*$ system, as well as their twin partners in the $B_s^*\bar{B}/B_s\bar{B}^*$ and $B_s^*\bar{B}^*$ systems under the heavy quark symmetry. Searching for these states would help us to assemble the jigsaw puzzles of dynamical details of the *hadronic molecular physics*.

II. EFFECTIVE POTENTIALS AND PRODUCTION AMPLITUDES

Since these states are produced near the corresponding thresholds, the interaction potential of a $\mathtt{VP}$ system ($\mathtt{V}$ and $\mathtt{P}$ denote the vector and pseudoscalar mesons, respectively) with the fixed isospin can be parametrized in the nonrelativistic form,

$$\mathcal{V}=\sum_{i=1}^{6}V_i(\boldsymbol{p}',\boldsymbol{p})\mathcal{O}_i(\boldsymbol{p}',\boldsymbol{p},\boldsymbol{\varepsilon},\boldsymbol{\varepsilon}^\dagger), \tag{1}$$

where $\boldsymbol{p}$ and $\boldsymbol{p}'$ represent the momenta of initial and final states in the center-of-mass system (c.m.s), respectively. $\boldsymbol{\varepsilon}$ and $\boldsymbol{\varepsilon}^\dagger$ denote the polarization vectors of the initial and final vector mesons, respectively. V_i are the scalar functions to be obtained from the chiral Lagrangians, while $\mathcal{O}_i$ are six pertinent operators,

$$\begin{aligned}
&\mathcal{O}_1=\boldsymbol{\varepsilon}^\dagger\cdot\boldsymbol{\varepsilon}, \qquad \mathcal{O}_2=(\boldsymbol{\varepsilon}^\dagger\times\boldsymbol{\varepsilon})\cdot(\boldsymbol{q}\times\boldsymbol{k}),\\
&\mathcal{O}_3=(\boldsymbol{q}\cdot\boldsymbol{\varepsilon}^\dagger)(\boldsymbol{q}\cdot\boldsymbol{\varepsilon}), \qquad \mathcal{O}_4=(\boldsymbol{k}\cdot\boldsymbol{\varepsilon}^\dagger)(\boldsymbol{k}\cdot\boldsymbol{\varepsilon}),\\
&\mathcal{O}_5=(\boldsymbol{q}\times\boldsymbol{\varepsilon}^\dagger)\cdot(\boldsymbol{q}\times\boldsymbol{\varepsilon}), \qquad \mathcal{O}_6=(\boldsymbol{k}\times\boldsymbol{\varepsilon}^\dagger)\cdot(\boldsymbol{k}\times\boldsymbol{\varepsilon}),
\end{aligned} \tag{2}$$

with $\boldsymbol{q}=\boldsymbol{p}'-\boldsymbol{p}$ the transferred momentum and $\boldsymbol{k}=(\boldsymbol{p}'+\boldsymbol{p})/2$ the average momentum.

Within the framework of χEFT, the potential up to the next-to-leading order (NLO) in the paired $\bar{D}_sD^*/\bar{D}_s^*D$ system can be classified as the contact interaction, one-eta-exchange (OEE) and two-kaon-exchange (TKE) contributions. The contact potential $\mathcal{V}_{\rm ct}$ is parametrized order by order in power series of $\boldsymbol{q}$ and $\boldsymbol{k}$ as

$$\mathcal{V}_{\rm ct}=(C_0+C_1\boldsymbol{q}^2+C_2\boldsymbol{k}^2)\mathcal{O}_1+\sum_{i=2}^{6}C_{i+1}\mathcal{O}_i+\ldots, \tag{3}$$

where C_i $(i=0,\ldots,7)$ are the unknown low energy constants (LECs), and the ellipsis denotes the higher order terms.

The effective potentials arising from the OEE and TKE contributions can be extracted from the LO chiral Lagrangians,

$$\begin{aligned}
\mathcal{L}=&\,i\langle\mathcal{H}v\cdot\mathcal{D}\bar{\mathcal{H}}\rangle+g\langle\mathcal{H}\gamma^\mu\gamma_5u_\mu\bar{\mathcal{H}}\rangle\\
&-i\langle\bar{\tilde{\mathcal{H}}}v\cdot\mathcal{D}\tilde{\mathcal{H}}\rangle+g\langle\bar{\tilde{\mathcal{H}}}\gamma^\mu\gamma_5u_\mu\tilde{\mathcal{H}}\rangle,
\end{aligned} \tag{4}$$

where the covariant derivative $\mathcal{D}_\mu=\partial_\mu+\Gamma_\mu$. The $\mathcal{H}$ and $\tilde{\mathcal{H}}$ denote the superfields of the charmed and anticharmed mesons, respectively. One can consult Refs. [33,35,36] for their expressions. The axial coupling $g\simeq0.57$ is extracted from the partial decay width of $D^{*+}\to D^0\pi^+$ [2]. The chiral connection Γ_μ and axial-vector current u_μ are formulated as

$$\Gamma_\mu\equiv\frac{1}{2}[\xi^\dagger,\partial_\mu\xi], \qquad u_\mu\equiv\frac{i}{2}\{\xi^\dagger,\partial_\mu\xi\}, \tag{5}$$

where $\xi^2=U=\exp(i\varphi/f_\varphi)$, with φ the normally used matrix form of the light Goldstone octet [33], and the decay constants $f_K=113$ and $f_\eta=116$ MeV (this is the normalization in which $f_\pi=92.4$ MeV), respectively.

Now, the quantum number $I^G(J^{PC})=1^+(1^{+-})$ for the Z_c state is favored [2] (C parity for the neutral one). The J^P quantum number of the Z_{cs} is undetermined, but $I(J^P)=\frac{1}{2}(1^+)$ is presumably used in most works [1,3,4,6]. Under this assumption, the flavor wave function of the Z_{cs} reads [3]

$$|Z_{cs}^-\rangle=\frac{1}{\sqrt{2}}(|D_s^{*-}D^0\rangle+|D_s^-D^{*0}\rangle). \tag{6}$$

One can easily get the OEE potential,

$$\mathcal{V}_{\rm OEE}=-\frac{g^2}{6f_\eta^2}\frac{\mathcal{O}_3}{\boldsymbol{q}^2+m_\eta^2}, \tag{7}$$

where m_η is the η meson mass, and $\boldsymbol{q}^2=p^2+p'^2-2pp'\cos\vartheta$ ($p=|\boldsymbol{p}|$, $p'=|\boldsymbol{p}'|$, and ϑ is the scattering angle in the c.m.s of $\mathtt{VP}$).

The TKE potential from the loop diagrams (see Ref. [15] for the involved loop diagrams and Refs. [31,36] for the calculation details) can be simplified into a compact form in the heavy quark limit and $\mathrm{SU}(3)_f$ limit,

$$\mathcal{V}_{\rm TKE}=V_1\mathcal{O}_1, \tag{8}$$

with

$$V_1 = -\frac{24(4g^2+1)m_K^2+(38g^2+5)\boldsymbol{q}^2}{2304\pi^2 f_K^4} + \frac{6(6g^2+1)m_K^2+(10g^2+1)\boldsymbol{q}^2}{768\pi^2 f_K^4}\ln\frac{m_K^2}{(4\pi f_K)^2} + \frac{4(4g^2+1)m_K^2+(10g^2+1)\boldsymbol{q}^2}{384\pi^2 f_K^4 y}\varpi\arctan\frac{y}{\varpi}, \quad (9)$$

where $\varpi=\sqrt{\boldsymbol{q}^2+4m_K^2}$ and $y=\sqrt{2pp'\cos\vartheta-p^2-p'^2}$. This result is obtained with the dimensional regularization, and the divergence is absorbed by the unrenormalized LECs introduced in Eq. (3).

The Z_{cs} state is observed in the three-body decay of $e^+e^-\to\gamma^*\to K^+(D_s^-D^{*0}+D_s^{*-}D^0)$. By fitting the line shape of the K^+ recoil-mass spectrum, we can extract the resonance parameters and pin down the inner structure of this state. The reaction is illustrated in Fig. 1, where the diagrams 1(a) and 1(b) depict the direct production and rescattering effect, respectively. The rescattering in Fig. 1(b) can generate the Z_{cs} state dynamically. Additionally, we construct the following effective Lagrangians to mimic the $\gamma^*\to K\mathtt{VP}$ coupling vertex:

$$\mathcal{L}_{\gamma^*\varphi VP} = g_\gamma\mathcal{F}^{\mu\nu}[(\tilde{P}_\mu^\dagger u_\nu P^\dagger-\tilde{P}_\nu^\dagger u_\mu P^\dagger) - (\tilde{P}^\dagger u_\mu P_\nu^\dagger-\tilde{P}^\dagger u_\nu P_\mu^\dagger)]+\text{H.c.}, \quad (10)$$

where g_γ denotes the effective coupling constant and $\mathcal{F}^{\mu\nu}$ is the field strength tensor of the virtual photon. $(\tilde{P}_\mu/\tilde{P})P_\mu/P$ denote the (anti)charmed vector/pseudoscalar meson fields (e.g., see Ref. [33]). u_μ is the axial-vector field defined in Eq. (5).

With the above effective potentials, the $K\mathtt{VP}$ production amplitude $\mathcal{U}(E,\boldsymbol{p})$ can be obtained by solving the following Lippmann-Schwinger equation (LSE):

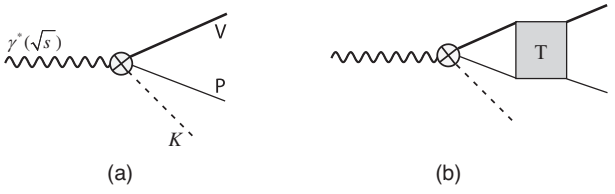

FIG. 1. Diagrams (a) and (b) describe the direct production and rescattering contribution, respectively. The wiggly, thick, thin, and dashed lines denote the virtual photon, vector meson, pseudoscalar meson, and kaon, respectively. The gray circle with cross stands for the effective $\gamma^*\to K\mathtt{VP}$ coupling, while the gray box in diagram (b) signifies the rescattering T matrix of the $\mathtt{VP}$ system.

$$\mathcal{U}(E,\boldsymbol{p}) = \mathcal{M}(E,\boldsymbol{p}) + \int\frac{d^3\boldsymbol{q}}{(2\pi)^3}\mathcal{V}(E,\boldsymbol{p},\boldsymbol{q})\mathcal{G}(E,\boldsymbol{q})\mathcal{U}(E,\boldsymbol{q}), \quad (11)$$

where $\mathcal{M}(E,\boldsymbol{p})$ represents the direct production amplitude of $\gamma^*\to K\mathtt{VP}$ described in Eq. (10), E is the invariant mass of the $\mathtt{VP}$ pair. The two-body propagator $\mathcal{G}(E,\boldsymbol{q})$ of the intermediate state is given as

$$\mathcal{G}(E,\boldsymbol{q}) = \frac{2\mu}{\boldsymbol{p}^2-\boldsymbol{q}^2+i\epsilon}, \qquad |\boldsymbol{p}|=\sqrt{2\mu(E-m_{\text{th}})}, \quad (12)$$

with μ and m_{th} the reduced mass and threshold of the $\mathtt{VP}$ system, respectively. In the calculation, we introduce the Gaussian form factor $\exp(-p'^2/\Lambda^2-p^2/\Lambda^2)$ (where Λ is the cutoff parameter) to avoid heavily involving the ultraviolet contributions [24,28,37].

The LSE of Eq. (11) is a three dimension integral equation, which can be reduced to one dimension through the partial wave decomposition. For example, the effective potentials in Eqs. (3) and (7)–(9) can be projected into the $|\ell sj\rangle$ basis (where ℓ, s, and j represent the orbital angular momentum, total spin, and total angular momentum of the $\mathtt{VP}$ system, respectively) via [38]

$$\mathcal{V}_{\ell,\ell'} = \int d\hat{\boldsymbol{p}}'\int d\hat{\boldsymbol{p}}\sum_{m_{\ell'}=-\ell'}^{\ell'}\langle\ell',m_{\ell'};s,m_j-m_{\ell'}|j,m_j\rangle \times\sum_{m_\ell=-\ell}^{\ell}\langle\ell,m_\ell;s,m_j-m_\ell|j,m_j\rangle\mathcal{Y}^*_{\ell'm_{\ell'}}(\theta',\phi') \times\mathcal{Y}_{\ell m_\ell}(\theta,\phi)\langle s,m_j-m_{\ell'}|\mathcal{V}|s,m_j-m_\ell\rangle, \quad (13)$$

with $\mathcal{Y}_{\ell m_\ell}$ the spherical harmonics. We have demonstrated that the S-D wave mixing effect is insignificant for the $Z_Q^{(\prime)}$ states [15], so we only consider the S-wave interaction for the Z_{cs} state in this paper. The contact interaction in the S-wave projection reads

$$\mathcal{V}_{\text{ct}} = \tilde{C}_{\text{s}} + C_{\text{s}}(p^2+p'^2), \quad (14)$$

where $\tilde{C}_s$ and C_s are the so-called partial wave LECs. They are the linear combinations of the LECs introduced in Eq. (3).

The differential decay width for $\gamma^*\to K\mathtt{VP}$ can be expressed in terms of the production amplitude in Eq. (11) as

$$\frac{d\Gamma}{dE} = \frac{1}{12(\sqrt{s})^2(2\pi)^3}|\mathcal{U}(E)|^2|\boldsymbol{k}_1||\boldsymbol{k}_2^*|, \quad (15)$$

where $\sqrt{s}$ is the c.m.s energy of the e^+e^- collision. $\boldsymbol{k}_1$ and $\boldsymbol{k}_2^*$ are the three momentum of the spectator K in the c.m.s

of e^+e^- and the three momentum of P(V) in the c.m.s of VP, respectively.

III. NUMERICAL RESULTS AND DISCUSSIONS

We study the $d\Gamma/dE$ distributions and extract the resonance parameters of the Z_{cs} state. The general procedure is to fit the K^+ recoil-mass spectrum measured by the BESIII Collaboration [1]. We essentially have three free parameters $\tilde{C}_{\rm s}$, $C_{\rm s}$, and Λ that can be varied to match the K^+ recoil-mass spectrum. In our previous work [15], these three parameters are well fixed by fitting the D^0D^{*-} invariant mass distributions of the Z_c state [39] (the double D tag technique is used in this experimental analysis, in which the background contribution is largely suppressed). When the values of LECs and cutoff in Ref. [15] are fed into the $D_s^-D^{*0}/D_s^{*-}D^0$ systems, we find a sharp peak automatically emerges around 3.98 GeV in the $D_s^{*-}D^0$ invariant mass spectrum. The result is shown in Fig. 2, where the blue dashed line is the production contribution in Fig. 1. When the other incoherent contributions in experiments are added up, the total line shape can quantitatively describe the distributions of experimental events (the red solid line in Fig. 2 with $\chi^2/\text{d.o.f} \simeq 0.67$). In other words, we can describe these two states in an uniform framework with the same set of parameters, which strongly supports that the Z_{cs} and Z_c states are partners in $\mathrm{SU}(3)_f$ symmetry.

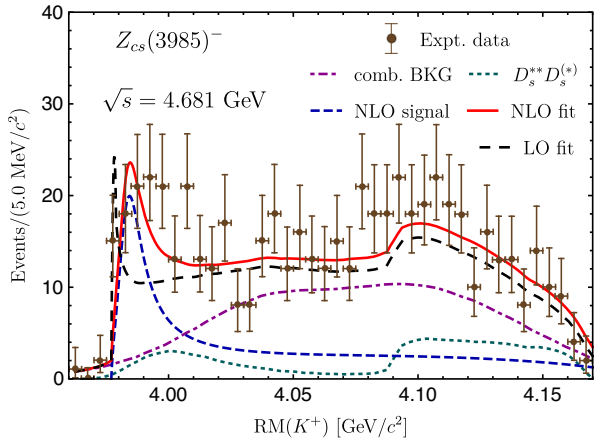

FIG. 2. The fit of the K^+ recoil-mass spectrum distributions in the $e^+e^- \to K^+(D_s^-D^{*0} + D_s^{*-}D^0)$ transitions. The data with error bars are taken from Ref. [1] at $\sqrt{s} = 4.681$ GeV. The red solid, blue dashed, purple dot-dashed, cyan dotted, and black dashed lines denote the NLO fit, signal contribution with NLO potentials, combinatorial background, $D_s^{**}D_s^{(*)}$ contributions (extracted from the experimental measurements), and LO fit (LO contact plus OEE), respectively. The line shape of the signal is obtained using the fitted parameters of $Z_c(3900)$ in Ref. [15] as inputs, i.e., $\tilde{C}_{\rm s} = 3.6 \times 10^2$ GeV^{-2}, $C_{\rm s} = -7.69 \times 10^3$ GeV^{-4}, and $\Lambda = 0.33$ GeV (where the central values in Ref. [15] are used).

We have tried to refit the experimental data of Ref. [1] and find the result is very similar. The line shape is slightly shifted and the parameters have similar size but just with a little larger errors (with $\chi^2/\text{d.o.f.} \simeq 0.64$). So the outputs are given in terms of the fitted parameters of the Z_c state in Ref. [15].

The fit with the LO potentials alone (LO contact terms plus the OEE) cannot reproduce the experimental data well (the black dashed line in Fig. 2 with $\chi^2/\text{d.o.f.} = 1.21$) and cannot describe the event distributions around 3.98 GeV. Including the NLO contributions in effective potential gives rise to a resonance peak, which conforms to the bump structure around 3.98 GeV in experiments. The improvement of the fitting indicates that the χEFT in the hidden charm sector tends to be convergent.

The peak lies above the $D_s^{*-}D^0$ threshold, which corresponds to a pole of the production $\mathcal{U}$ matrix in the unphysical Riemann sheet. This can be conducted through analytical continuation of the Green's function $\mathcal{G}$ defined in Eq. (12),

$$\mathcal{G}^b(p + i\epsilon) \equiv \mathcal{G}^a(p + i\epsilon) - 2i\mathrm{Im}\mathcal{G}^a(p + i\epsilon), \quad (16)$$

where $\mathcal{G}^a$ and $\mathcal{G}^b$ denote the Green's function defined in the physical and unphysical Riemann sheets, respectively. The pole position $m - i\Gamma/2$ reads

$$(m, \Gamma) = (3982.4^{+4.8}_{-3.4}, 11.8^{+5.5}_{-5.2})\ \text{MeV}, \quad (17)$$

where the errors inherit from those of the fitted parameters in Ref. [15]. The mass and width are highly consistent with the experimental data [1]. Therefore, our studies strongly support the Z_c and Z_{cs} as the $\mathrm{SU}(3)_f$ symmetry parters and the resonances generated from the $D\bar{D}^*/\bar{D}D^*$ and $\bar{D}_sD^*/\bar{D}_s^*D$ interactions, respectively.

In addition, the formations and decay properties of these resonances can be synchronously interpreted in the molecular configuration pictures (the compact tetraquarks do not necessarily require their masses reside very close to the threshold). The near-threshold production indicates the V and P(V) mesons move very slowly, which renders them have enough time to interact with each other. A strongly attractive interaction can confine two particles for infinite time, which corresponds to a stable bound state. If the attraction is not enough strong but with a barrier to trap two particles for a finite time, then a resonance with certain lifetime is generated. In contrast to the bound states, the resonances naturally decompose into their ingredients at the end of their lifetime, i.e., the elastic decay modes would contribute dominantly to the partial decay widths. Yet, the inelastic decays with final states of a heavy quarkonium and a light meson proceed via shorter distance interactions (with $r \sim 1/m_D$), which are generally suppressed and thus react with less probability. Thus, the inelastic channels only contribute a small amount of the partial widths [11,13].

TABLE I. The resonance information of $Z_{cs}(3985)$ [1] and other predicted states in the $\bar{D}_s^* D^*$, $B_s^* \bar{B}/B_s \bar{B}^*$, and $B_s^* \bar{B}^*$ systems. The superscript "†" means this state has been observed, while the unobserved states are marked with boldface. We define the masses and widths of the resonances from their pole positions $E = m - i\Gamma/2$ (with m the mass and Γ the width). The Δm represents the distance between the resonance and its threshold, i.e., $\Delta m = m - m_{\rm th}$.

Systems	$I(J^P)$	Thresholds (MeV)	Masses (MeV)	Widths (MeV)	Δm (MeV)	States
$\frac{1}{\sqrt{2}}[\bar{D}_s^* D + \bar{D}_s D^*]$	$\frac{1}{2}(1^+)$	3977.0	$3982.5^{+1.8}_{-2.6} \pm 2.1$	$12.8^{+5.3}_{-4.4} \pm 3.0$	$5.5^{+1.8}_{-2.6} \pm 2.1$	$Z_{cs}(3985)^\dagger$
$\bar{D}_s^* D^*$	$\frac{1}{2}(1^+)$	4119.1	$4124.2^{+5.6}_{-3.7}$	$9.8^{+5.2}_{-4.8}$	$5.1^{+5.6}_{-3.7}$	$\boldsymbol{Z_{cs}(4125)}$
$\frac{1}{\sqrt{2}}[B_s^* \bar{B} + B_s \bar{B}^*]$	$\frac{1}{2}(1^+)$	10694.7	$10701.9^{+3.9}_{-2.7}$	$7.4^{+3.6}_{-4.4}$	$7.2^{+3.9}_{-2.7}$	$\boldsymbol{Z_{bs}(10700)}$
$B_s^* \bar{B}^*$	$\frac{1}{2}(1^+)$	10740.1	$10747.0^{+4.3}_{-3.1}$	$7.3^{+3.7}_{-4.6}$	$6.9^{+4.3}_{-3.1}$	$\boldsymbol{Z_{bs}(10745)}$

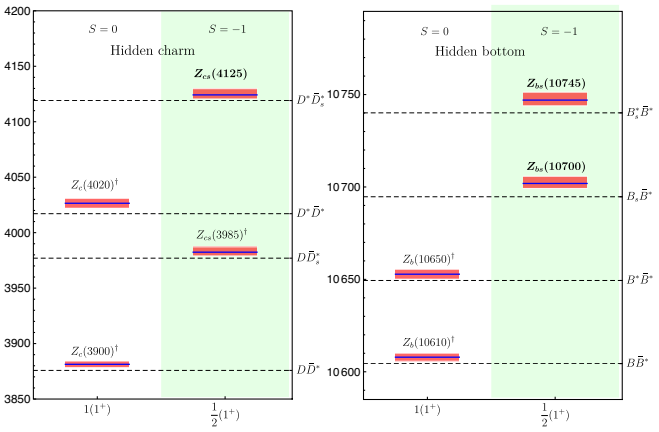

FIG. 3. A complete spectrum of the charged charmoniumlike (left panel) and bottomoniumlike (right panel) states with strangeness $S = 0$ and $S = -1$, respectively. The blue solid lines and red bands denote the central values and range of errors of the masses, respectively. The observed and predicted states are marked with † and boldface, respectively.

We can adopt the same framework to predict the unobserved states in the $\bar{D}_s^* D^*$ system as well as the $B_s^* \bar{B}/B_s \bar{B}^*$ and $B_s^* \bar{B}^*$ systems in the hidden bottom sectors. The inputs for these systems come from the fitted parameters of the Z_c', Z_b and Z_b' states in Ref. [15], respectively. The predictions are listed in Table I. We find that there indeed exists a resonance in the $\bar{D}_s^* D^*$ system and two resonances in the $B_s^* \bar{B}/B_s \bar{B}^*$ and $B_s^* \bar{B}^*$ systems, respectively. They lie around 5–7 MeV above the corresponding thresholds, and their widths coincide with those of the observed partners. Including the observed $Z_Q^{(\prime)}$ states, we can establish a complete spectrum for the $1(1^+)$ and $\frac{1}{2}(1^+)$ charged heavy quarkoniumlike states. The spectrum is vividly illustrated in Fig. 3. These predicted states could be reconstructed at the corresponding open charm/bottom channels or the $J/\psi K$ and $\Upsilon(nS)K$ $(n = 1, 2)$ final states, respectively. Hunting for these states would be an intriguing topic in future experiments.

IV. SUMMARY AND OUTLOOK

In summary, we have generalized the framework of χEFT to decode the nature of the newly observed exotic Z_{cs} state by BESIII [1]. The proximity to the $\bar{D}_s D^*/\bar{D}_s^* D$ threshold and large similarity with Z_c hint that this unusual state may be a cousin of the Z_c in $\mathrm{SU}(3)_f$ family. The interaction kernel of the $\bar{D}_s D^*$ system is calculated up to the NLO, which incorporates the LO contact terms, OEE and the NLO contact terms, and TKE. When the LECs and cutoff fitted from the Z_c data are fed into the Z_{cs}, iterating the effective potential in LSE automatically generates a sharp peak near the $\bar{D}_s D^*/\bar{D}_s^* D$ threshold in the $\bar{D}_s D^*$ invariant mass spectrum. The mass and width from the pole of the production $\mathcal{U}$ matrix are very consistent with the experimental data, and the distributions of events can also be well described. Our studies strongly support that the Z_{cs} and Z_c are partners in $\mathrm{SU}(3)_f$ family, and they have the same dynamical origin. Inspired by the Z_{cs} results, we also predict the resonance parameters of three unobserved states in the $\bar{D}_s^* D^*$, $B_s^* \bar{B}/B_s \bar{B}^*$, and $B_s^* \bar{B}^*$ systems. We have established a complete spectrum of the charged charmoniumlike and bottomoniumlike states. Looking for these predicted states in experiments would help us to understand the chiral dynamics, the manifestations of $\mathrm{SU}(3)_f$ and heavy quark symmetries at the hadron levels, more deeply.

ACKNOWLEDGMENTS

This project was supported by the National Natural Science Foundation of China under the Grant No. 11975033. This work was supported in part by DFG and NSFC through funds provided to the Sino-German CRC 110 "Symmetries and the Emergence of Structure in QCD."

[1] M. Ablikim *et al.* (BESIII Collaboration), arXiv:2011.07855.
[2] P. A. Zyla *et al.* (Particle Data Group), Prog. Theor. Exp. Phys. (**2020**), 083C01.
[3] L. Meng, B. Wang, and S. L. Zhu, arXiv:2011.08656.
[4] Z. Yang, X. Cao, F. K. Guo, J. Nieves, and M. P. Valderrama, arXiv:2011.08725.
[5] J. Z. Wang, Q. S. Zhou, X. Liu, and T. Matsuki, arXiv:2011.08628.
[6] B. D. Wan and C. F. Qiao, arXiv:2011.08747.
[7] M. C. Du, Q. Wang, and Q. Zhao, arXiv:2011.09225.
[8] R. Chen and Q. Huang, arXiv:2011.09156.
[9] X. Cao, J. P. Dai, and Z. Yang, arXiv:2011.09244.
[10] Z. F. Sun and C. W. Xiao, arXiv:2011.09404.
[11] M. Ablikim *et al.* (BESIII Collaboration), Phys. Rev. Lett. **112**, 022001 (2014).
[12] M. Ablikim *et al.* (BESIII Collaboration), Phys. Rev. Lett. **115**, 182002 (2015).
[13] A. Garmash *et al.* (Belle Collaboration), Phys. Rev. Lett. **116**, 212001 (2016).
[14] N. Brambilla, S. Eidelman, C. Hanhart, A. Nefediev, C. P. Shen, C. E. Thomas, A. Vairo, and C. Z. Yuan, Phys. Rep. **873**, 1 (2020).
[15] B. Wang, L. Meng, and S. L. Zhu, Phys. Rev. D **102**, 114019 (2020).
[16] H. X. Chen, W. Chen, X. Liu, and S. L. Zhu, Phys. Rep. **639**, 1 (2016).
[17] F. K. Guo, C. Hanhart, U. G. Meißner, Q. Wang, Q. Zhao, and B. S. Zou, Rev. Mod. Phys. **90**, 015004 (2018).
[18] Y. R. Liu, H. X. Chen, W. Chen, X. Liu, and S. L. Zhu, Prog. Part. Nucl. Phys. **107**, 237 (2019).
[19] R. F. Lebed, R. E. Mitchell, and E. S. Swanson, Prog. Part. Nucl. Phys. **93**, 143 (2017).
[20] A. Esposito, A. Pilloni, and A. D. Polosa, Phys. Rep. **668**, 1 (2017).
[21] E. Braaten and H.-W. Hammer, Phys. Rep. **428**, 259 (2006).
[22] V. Bernard, N. Kaiser, and U. G. Meißner, Int. J. Mod. Phys. E **04**, 193 (1995).
[23] E. Epelbaum, H. W. Hammer, and U. G. Meißner, Rev. Mod. Phys. **81**, 1773 (2009).
[24] R. Machleidt and D. R. Entem, Phys. Rep. **503**, 1 (2011).
[25] E. Epelbaum, H. Krebs, and P. Reinert, Front. Phys. **8**, 98 (2020).
[26] U. G. Meißner, Phys. Scr. **91**, 033005 (2016).
[27] H.-W. Hammer, S. König, and U. van Kolck, Rev. Mod. Phys. **92**, 025004 (2020).
[28] D. Rodriguez Entem, R. Machleidt, and Y. Nosyk, Front. Phys. **8**, 57 (2020).
[29] S. Weinberg, Phys. Lett. B **251**, 288 (1990).
[30] S. Weinberg, Nucl. Phys. **B363**, 3 (1991).
[31] B. Wang, L. Meng, and S. L. Zhu, J. High Energy Phys. 11 (2019) 108.
[32] L. Meng, B. Wang, G. J. Wang, and S. L. Zhu, Phys. Rev. D **100**, 014031 (2019).
[33] B. Wang, L. Meng, and S. L. Zhu, Phys. Rev. D **101**, 034018 (2020).
[34] M. Z. Wang, Recent results on exotic hadrons at LHCb.
[35] M. B. Wise, Phys. Rev. D **45**, R2188 (1992).
[36] B. Wang, Z. W. Liu, and X. Liu, Phys. Rev. D **99**, 036007 (2019).
[37] E. Epelbaum, W. Glockle, and U. G. Meissner, Nucl. Phys. **A747**, 362 (2005).
[38] J. Golak *et al.*, Eur. Phys. J. A **43**, 241 (2010).
[39] M. Ablikim *et al.* (BESIII Collaboration), Phys. Rev. D **92**, 092006 (2015).